

## EFFECT OF LOW-PERMEABILITY SOIL LAYERS ON THE STABILITY OF SUBMARINE SLOPES

Pradipta Chakraborty, Faculty of Engineering & Applied Science, Memorial University, St. John's, NL,  
Ahmad Jafari Mehrabadi – Faculty of Engineering & Applied Science, Memorial University  
Radu Popescu – Faculty of Engineering & Applied Science, Memorial University

### ABSTRACT

This paper presents a numerical study of the effects of low-permeability layers on the stability of submarine slopes. The numerical model used in this study is the multi-yield plasticity soil constitutive model implemented in the finite element program DYNAFLOW. The phenomenon is first analyzed at small scale by numerically simulating a series of laboratory cyclic undrained tests performed on uniform and layered soil samples. It is concluded that migration of water from softer, more permeable layers into sand layers may significantly reduce liquefaction resistance. Next, fully coupled, effective stress non-linear dynamic analyses of submarine slopes, both with and without low-permeability layers are carried out and the results are compared to show the significant influence of those layers on the behavior of such slopes.

### RÉSUMÉ

Cet article présente une étude numérique des effets des couches de bas-perméabilité sur la stabilité des pentes submersibles. Le phénomène est d'abord analysé à la petite échelle en simulant numériquement une série des essais de laboratoire. Après, des analyses dynamiques non linéaires d'effort entièrement couplé et efficace des pentes submersibles, avec et sans des couches de bas-perméabilité sont effectuées et les résultats sont comparés pour montrer l'influence significative de ces couches sur le comportement de telles pentes.

### 1. INTRODUCTION

Many natural soils and man-made sand deposits include low-permeability silty or clayey layers. During earthquakes water may be trapped beneath a stratum of relatively low permeability. This forms a water-rich seam beneath such a layer causing reduction of shear strength of soil along the seam. If drainage is hindered for a long time after earthquake, delayed flow failure and large displacements may take place after the end of shaking. For example, the Lower San Fernando Dam near Los Angeles, slope failure took place 1 min after shaking stopped during San Fernando earthquake (Seed 1987).

Several studies have been reported this phenomenon of water film formation. Fiegel et al (Fiegel et al, 1994) reported this phenomenon during a centrifuge experiment with layered soil. Kokusho (Kokusho, 1999, 2000a, 2000b) observed the formation of water film during a shake table test. Although this water film has a quite significant influence in soil liquefaction only limited work has been done to further understand its effects.

From earlier work it is clear that if an impermeable silt or clay layer is present in sand then liquefaction resistance of that layered sand is much less than that of the clean sand. Kokusho and Kojima (Kokusho and Kojima 2002) concluded from their experiment that liquefaction of layered sand is associated with the presence of a water film beneath a less pervious layer due to the local migration of pore water. Konrad and Dubeau (Konrad and Dubeau 2002) performed a series of undrained cyclic triaxial tests on uniform sand, uniform silt and layered soil (sand and silt

layers). From the result they concluded that the cyclic strength of the stratified sand-silt samples was decreased considerably when compared to that of 100% sand or 100% silt sample at the same void ratio and subjected to identical undrained cyclic loads.

In the present study the multi-yield plasticity soil constitutive model implemented in the finite element program DYNAFLOW (Prevost 2002) is used to numerically simulate the undrained triaxial tests performed by Konrad and Dubeau (2002). First, the multi-yield plasticity model parameters are calibrated by simulating some undrained triaxial tests and comparing the results with those obtained by Konrad and Dubeau. This model calibration is done for both uniform sand and uniform silt samples. After calibration of the model an undrained triaxial test is numerically simulated for the layered sample. Next, fully coupled effective stress non-linear dynamic analyses of submarine slope (both with and without silt layer) are carried out and the results are compared to show the influence of those layers to the failure of such slope due to liquefaction.

### 2. MULTI-YIELD PLASTICITY SOIL CONSTITUTIVE MODEL

The constitutive model used in this study is the multi-yield plasticity soil constitutive model implemented in the finite element code DYNAFLOW. This model has been validated several times in the past for analysis of liquefaction phenomenon (Popescu and Prevost 1993, 1995). The model is a kinematic hardening model based on a relatively

simple plasticity theory (Prevost 1985), and is applicable to both cohesive and cohesionless soils. Fundamental theory behind the model has originated from the concept of a “field of work-hardening moduli” (Mroz 1967) by approximating the nonlinear elastic plastic stress-strain curve into a number of linear segments with constant shear moduli. This results in defining a series of nested yield surfaces in the stress space. Each yield surface corresponds to a region of a constant shear modulus. The outermost surface is related to zero shear modulus, and is called failure surface. Both Drucker-Prager and Mohr-Coulomb type surfaces can be employed in the model for frictional materials (sands).

The plastic potential is assumed to be associative for its deviatoric component and non-associative for its dilatational (volumetric) component. The volumetric component is defined to account for dependence of soil dilatational behavior on the mobilized stress ratio. The soil hysteretic behavior and shear stress-induced anisotropic effects are simulated by a purely deviatoric kinematic hardening rule (Prevost 1989). Main features of the multi-yield plasticity soil constitutive model are shown in Figure 1 (Popescu 1995).

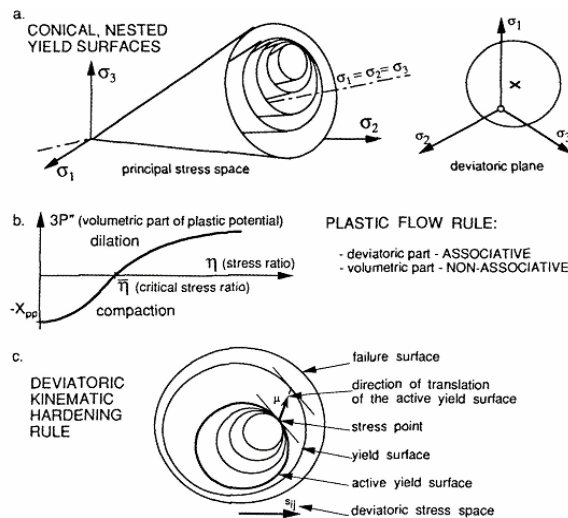


Figure 1. Main features of the multi-yield plasticity soil constitutive model(after Popescu 1995).

### 3. CALIBRATION OF CONSTITUTIVE PARAMETERS

The required soil constitutive parameters of the multi-yield plasticity model are listed in Table 1. Most of those parameters have been estimated using information in the literature and previous experience. The dilation parameter ( $X_{pp}$ ) that scales the shear induced plastic volumetric strain was estimated based on the results reported by Konrad and Dubeau (2002) for uniform sand and silt samples and liquefaction strength analysis (see e.g. Popescu and Prevost, 1993, for a detail description of the procedure). The experimental and predicted liquefaction strength curves are shown in Figure3.

Table 1. Constitutive parameters used in this study

Constitutive parameter	Symbol	Type	Sand	Silt
Mass density solid	$\rho^s$	State parameters	2670 kg/m <sup>3</sup>	2670 kg/m <sup>3</sup>
Porosity	$n^w$		0.363	0.46/0.44
Hydraulic conductivity	$k$		0.00013 m/s	10 <sup>-7</sup> m/s
Low strain elastic shear modulus	$G_0$	Low strain Elastic parameters	20Mpa	2Mpa
Poisson's ratio	$\nu$		0.2	0.4
Power exponent	$n$		0.5	0.8
Friction angle at failure	$\phi$	Yield and failure parameters	45	32 <sup>0</sup> / 33 <sup>0</sup>
Maximum deviatoric strain (comp/ext)	$\epsilon_{dev}^{max}$		0.06/ 0.04	0.10/ 0.08
Coefficient of lateral stress	$k_0$		1.0	1.0
Stress-strain curve coefficient	$\alpha$		0.19	--
Dilation angle	$\psi$		31 <sup>0</sup>	25 <sup>0</sup>
Dilation parameter	$X_{pp}$	Dilation parameters	0.006	0.0161

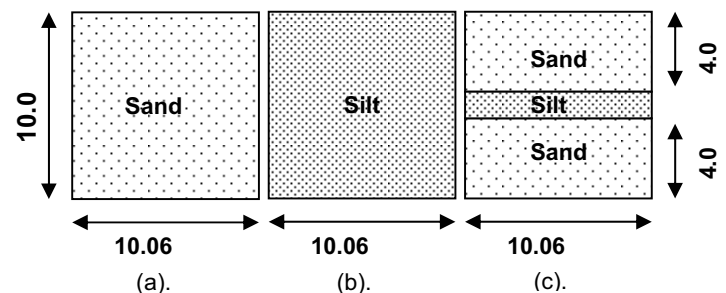


Figure 2. Schematic diagram of triaxial test samples (all dimensions are in cm)

### 4. NUMERICAL SIMULATIONS OF CYCLIC UNDRAINED TRIAXIAL TESTS OF LAYERED SAMPLES

Dimension of the samples are shown in Figure 2. The finite element mesh for layered sample is shown in Figure 4. Axisymmetric finite element simulation of undrained cyclic test of layered soil was performed at a cyclic stress ratio, CSR=0.166. The sample was predicted to liquefy after 56 cycles. Similarly to the laboratory experiments reported by Konrad and Dubeau (2002), the liquefaction strength of the uniform soil samples was predicted to be significantly higher (liquefaction after 98 cycles for the silt and after 150 cycles for the sand sample, both subjected to the same CSR as the layered soil sample). Pore water pressure contours are shown in Figure 5. Pore water pressure development in sand and silt with number of cycles are

shown in Figure 6. Slightly more pore water pressure build-up was predicted in the sand than in the silt. This is apparently due to movement of water in vertical direction relative to solid particles at the interface of sand and silt layer as shown in Figure 7. It is clear from the relative displacements shown in Figure 6 that water is migrating from the more compressible silt layer to the surrounding sand. This phenomenon may be similar to injection of small quantities of water during an undrained cyclic test that was proven to highly increase liquefaction potential.

Predicted axial strains in sand and silt are shown in Figure 8. It can be observed that liquefaction failure of the layered sample is predicted to take place in sand, when this reaches axial strains of about 15%, which are larger than the axial strain at failure in the uniform sand sample (12%). At this moment the silt still has not reached the "liquefaction strains" yet (38% in the uniform silt sample as compare to 17% in the layered sample).

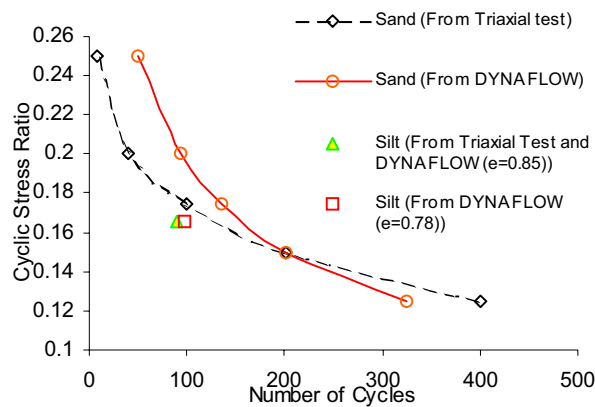


Figure 3. Liquefaction strength analysis

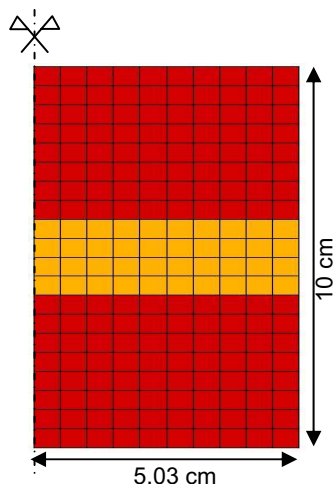


Figure 4. Finite Element Mesh of layered sample

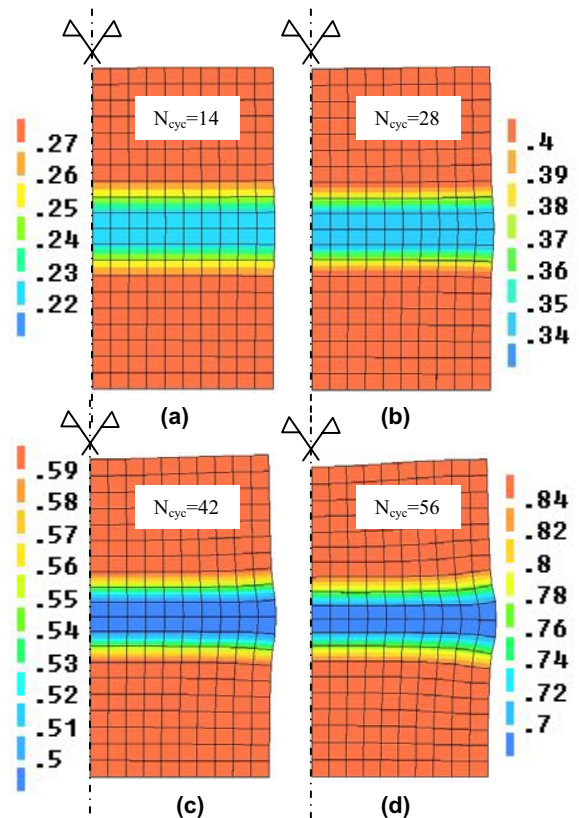


Figure 5. Predicted contours of excess pore water pressure ratio at different time instants. Deformation magnification factor = 2.

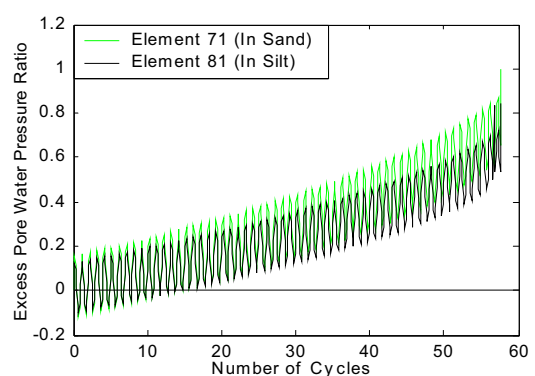


Figure 6. Predicted excess pore water pressure ratio in the layered sample

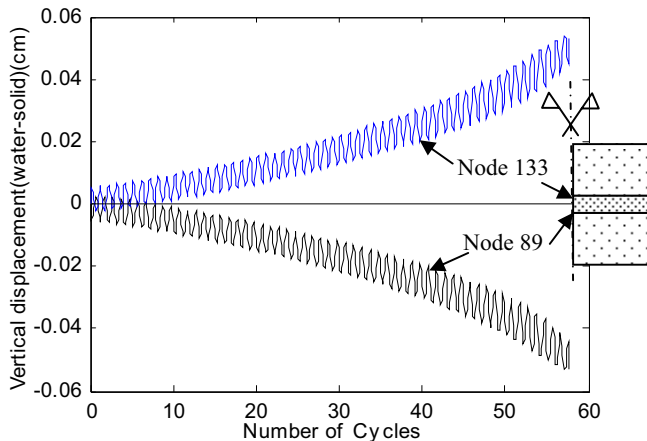


Figure 7. Predicted relative vertical displacement (water-solid) at the interface of silt and sand in the layered sample

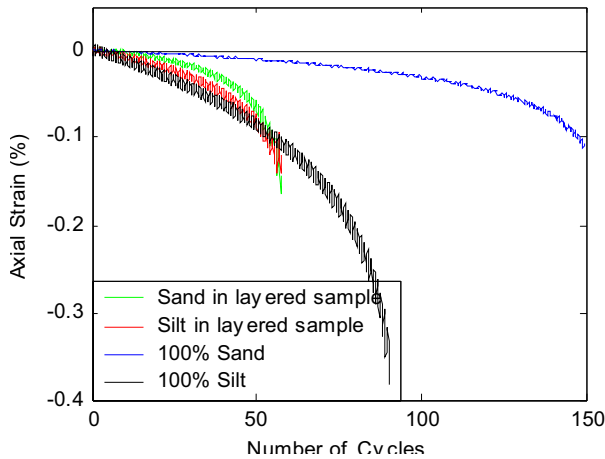


Figure 8. Predicted average axial strains for sand and silt

## 5. SEISMIC ANALYSIS OF A SUBMARINE SLOPE

The submarine slope analyzed here is shown in Figure 9. The finite element model consists of 450 four-node elements with 4 degrees of freedom per node, i.e. two for

solid and two for fluid displacements. The seismic motion is assumed to be a sinusoidal motion with a frequency of 1Hz and acceleration amplitude of 0.083 g to account for the range of cyclic stress ratios used in the laboratory soil tests discussed previously. The seismic motion is applied in horizontal direction at the base and lateral boundaries of the analysis domain. The base and lateral boundaries are assumed impervious. Three different models considered in this study include model 1, dense sand with a 2m-thick silt layer, model 2, dense sand only, and model 3, silt only. The top of the silt layer in model 1 is located at 2m below the ground surface as shown in Figure 9.

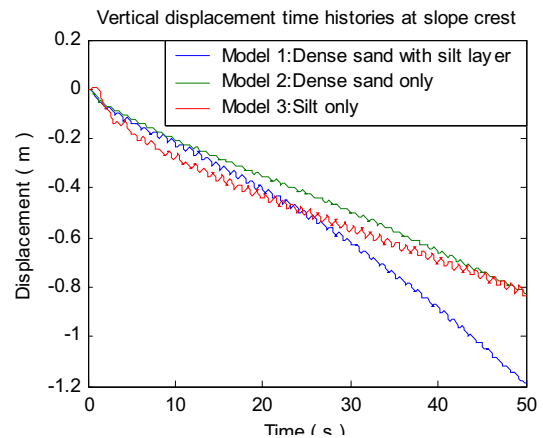


Figure 10. Predicted vertical displacement time histories at the slope crest

## 5.1 RESULTS AND DISCUSSION

Figure 10 shows the predicted vertical displacement time histories at the slope crest. As it can be seen from this figure, presence of the silt layer in model1 causes significant increase of about 50% in vertical settlement at the slope crest, i.e., from 0.8m for homogeneous slopes (models 2 and 3) to 1.2 m for model 1.

Figure 11 shows the predicted maximum shear strain contours along with the deformed shapes of the slope at  $t=50$  s (after 50 cycles). The silt layer in model 1 causes local failure surfaces at upper parts of the slope parallel to the silt layer.

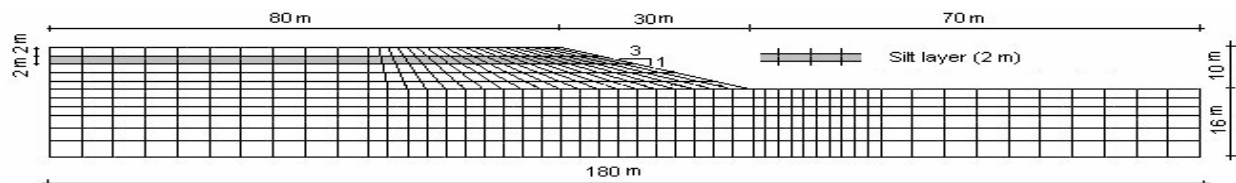


Figure 9. Geometry and finite element mesh of the earth slope used in this paper.

The 2m- thick silt layer shown in this figure exists only in model 1, i.e., dense sand with a silt layer. Soil in models 2 and 3 is assumed to be homogenous dense sand and silt , respectively.

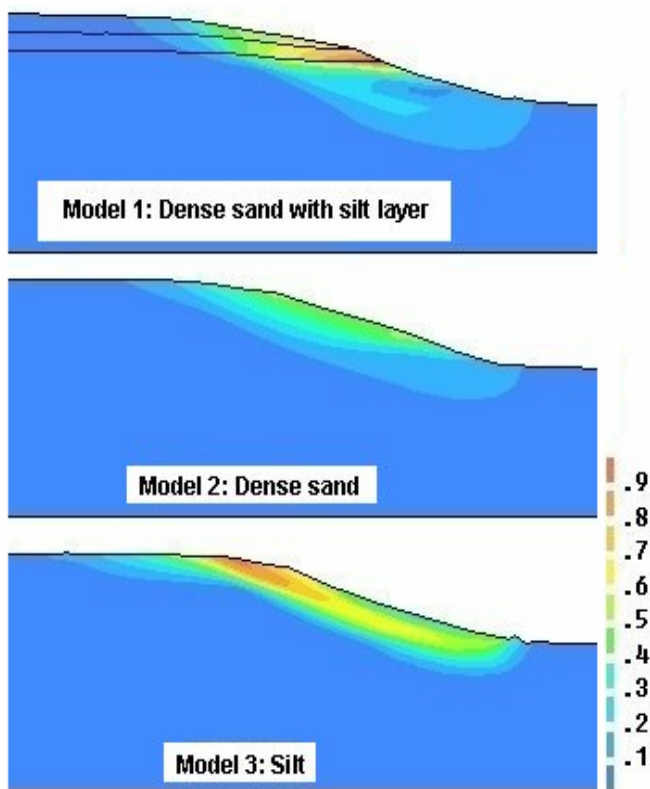


Figure 11. Predicted maximum shear strain contours after 50 cycles for models 1 to 3. Deformed shapes are shown with a magnification factor of 2. Only the central part of each model is shown.

## 6. CONCLUSIONS

From the present study it is concluded that the presence of low permeability layers diminish the liquefaction strength of a sand deposit. Excess pore water pressure in the sand with low permeability material inclusions increases more rapidly than in clean sand due to water migration from the low permeability layer. It causes early reduction in strength in the sand and may result in failure due to soil liquefaction.

## 7. ACKNOWLEDGEMENT

This research is financially supported by NSERC as part of a Liquefaction Remediation Initiative, COSTA Canada and Grant No. RG203795-02. This support is gratefully acknowledged.

## 8. REFERENCES

- Fiegel, G.L. and Kutter, B.L., 1994, "Liquefaction for layered soils", *Journal of Geotechnical and Geo-environmental engineering*, ASCE, Vol. 120, No. 4, pp. 737-755.
- Kokusho, T. 1999, "Formation of water film in liquefied sand and its effect on lateral spread", *Journal of Geotechnical and Geo-environmental Engineering*, American Society of Civil Engineers, Vol.125, No.10, pp.817-826.
- Kokusho, T. 2000a, "Mechanism for water film generation and lateral flow in liquefied sand layer", *Soils and Foundations*, Vol.40, No.5, pp.99-111.
- Kokusho, T. 2000b, "Emergence of water film in liquefied sand and its role in lateral flow", 12<sup>th</sup> World Conference on Earthquake Engineering (Auckland-New Zealand) CD-ROM 0946.
- Kokusho, T. and Kojima, T. 2002. "Mechanism for post liquefaction water film generation in layered sand", *Journal of Geotechnical and Geo-environmental engineering*, ASCE, Vol. 18, No 2, pp. 129-137.
- Konrad, J.M., and Dubeau, S., 2002. "Cyclic strength of stratified samples", *Proc. of the 55<sup>th</sup> Canadian Geotechnical and 3<sup>rd</sup> Joint IAH-CNC and CGS Groundwater Specialty Conferences*, Niagara Falls, Ontario, October 20-23, pp. 89-94.
- Mroz, Z., 1967. "On the behavior of anisotropic work-hardening". *J. Mech. Phys. Solids*, vol. 15, pp. 163-175.
- Popescu, R., 1995. "Stochastic variability of soil properties: Data Analysis, Digital Simulation, effects on system behavior", Ph.D. Thesis, Princeton University, Princeton, NJ
- Popescu, R., and Prevost, J.H., 1993. "Centrifuge validation of a numerical model for dynamic soil liquefaction", *Soil Dynamics and Earthquake Engineering*, vol. 12(2), pp. 73-90.
- Popescu, R., and Prevost, J.H., 1995 "Comparison between VELACS numerical class 'A' predictions and centrifuge experimental soil test results", *Soil Dynamics and Earthquake Engineering*, vol. 14(2), pp. 79-92.
- Prevost, J.H., (1985). "A simple plasticity theory for frictional cohesionless soils", *Soil Dynamics and Earthquake Engineering*, 4(1): 9-17.
- Prevost, J.H., 1989. "DYNA1D, a computer program for nonlinear seismic site response analysis", Technical report NCEER-89-0025. National Center for Earthquake Engineering research. State University of New York at Buffalo.
- Prevost, J.H. (2002). "Dynaflow - A nonlinear transient finite element analysis program", Version 02, Tech. Report, Dept. of Civil and Environmental Engineering, Princeton University, Princeton, NJ.
- Seed, H.B. 1987, "Design problems in soil liquefaction", *Journal of Geotechnical Engineering*, Vol.113, No.8, ASCE, 827-845.